

Thermal degradation of Tunisian olive stones using thermogravimetric analysis (TGA)

Amina Bedoui, Souad Souissi-Najar, and Abdelmottaleb Ouederni

Laboratory of Process Engineering and Industrial Systems (LR11ES54), National School of Engineers, University of Gabes,
Medenine Street 6029, Tunisia

Copyright © 2016 ISSR Journals. This is an open access article distributed under the **Creative Commons Attribution License**, which permits unrestricted use, distribution, and reproduction in any medium, provided the original work is properly cited.

ABSTRACT: The aim of this paper is to study of the thermal degradation of Tunisian olive stones by non-isothermal thermogravimetric analysis (TGA) device, under nitrogen atmosphere. Thermogravimetric analysis of different particles sizes (0.63-2.5mm) was evaluated. The effect of heating rates has been performed. Results showed that particles sizes don't have any effect on the pyrolysis of olive stones whereas the decomposition process is shifted to higher temperature zone with heating rate increasing. Three different kinetic models, the iso-conversional; kissinger-Akahira-Sunose, Ozawa-Flynn-Wall methods and Coats Redfern model were applied on TGA data of olive stones (OS) to calculate the kinetic parameters including activation energy, pre-exponential factor and reaction order. Simulation of olive stones pyrolysis using data obtained from TGA analysis showed good agreement with experimental data for all models. The dependence of the apparent activation energy determined using kissinger-Akahira-Sunose (KAS) and Ozawa-Flynn-Wall (OFW) methods, on the conversion degree reveals that pyrolysis progress rather through multi-steps kinetics.

KEYWORDS: TGA; thermal degradation; iso-conventional methods; Activation energy.

1 INTRODUCTION

Olive oil production is of great economical importance in many Mediterranean countries, i.e. Spain, Italy, Turkey, Greece, and Tunisia, that's present large producers that have together marketed 97% of the world olive oil production ([1], [2]). In 2012, Tunisia represent the fourth largest exporter of olive oil worldwide, with an export production of 163,000 tons, this amount was expected to increase in 2013 according to the General Directorate for Research at the Ministry of Agriculture [3]. Thus, the amount of bio-wastes produced by the olive oil industry is increasing that's well known that the production of olive oil generates large volumes of wastes.

Several researches prove that energetic valorization is the solution for the solid waste elimination ([4], [5], [6]). That's using biomass to produce bioenergy is often a way to dispose of waste materials that otherwise would create environmental risks. The energy exploitation of biomass is an interesting challenge since it is zero net CO₂ emission, it is unlimited, and it minimizes the disposal problems associated with the generation of agricultural by-products. Moreover, biomass exploitation allows the possibility of generating added value products such as chemicals or activated carbons (ACs) which means an attractive economic and technological solution.

Thermo-chemical conversion such as combustion, gasification, pyrolysis is the most commonly biomass conversion method to upgrade biomass energy quality ([4], [7], [8]). It has been widely reported the feasibility of using agricultural by-products as renewable source of energy by means of pyrolysis processes ([4], [8], [9], [10]). Pyrolysis is one of the most employed methods to convert biomass and organic residues into diverse products. Solid biomass and wastes, which are very difficult and costly to manage, can be readily converted into liquid, gas and charcoal products by the pyrolysis process. Therefore, research on the pyrolysis process of a specific ligno-cellulosic waste would be beneficial for a better understanding of the pyrolytic mechanism and to improve its transformation and application as bio-fuels, chemical products and bio-materials. So, among the many reasons for quantifying the rate of a chemical reaction, the thermo-kinetic behavior

of the biomass is of high importance during the degradation of its main components, which allow control the reaction rate as a function of temperature and composition.

Various procedures for evaluating kinetic parameters from data derived from non isothermal thermogravimetric analysis (TGA) have been developed, and the vast majority of them can be classified as either “model-free” or “model-fitting” ([8], [10], [11]). Recently, the model-free method, also called the iso-conversional method, was the most common used methods in the kinetics study of biomass pyrolysis process ([13], [14]). The model-free approach does not require assumption of specific reaction models, and yields unique kinetic parameters as a function of either conversion or temperature. According to which a single step process is considered and the need of accurate reaction scheme is eliminated.

Of the two main model free methods the iso-conversional approach is more frequently adopted, and is increasingly being used in biomass thermochemical conversion research. Recently, various iso-conversional methods are employed in the analysis of the non isothermal decomposition of biomasses ([4], [13], [14], [15]).

For olive stones, numerous studies on the TGA kinetic non-isothermal pyrolysis are available ([5], [10], [16], [17], [18]) and most were based on fitting models. La référence [18] studied pyrolysis kinetics of almond shells and olive stones considering their organic fractions and applicated the independent reactions model for calculating kinetic parameters. On the other hand, reaction kinetic parameters of olive waste are obtained under inert and oxidative conditions using global independent reactions model [5].

So that, the aim of the present paper is to characterize the olive stones and studying the kinetic of pyrolysis by the application of free (iso-conventionals) models. The Ozawa– Flynn–Wall (OFW) ([19], [20]) and the Kissinger– Akahira–Sunose (KAS) [21] kinetic models allow the calculation of the activation energy of the process. Coats-Redfern method will be used to determine the pre-exponential factor. The obtained results will be compared to the experimental in order to compare the validity and performance of the models.

The used data were obtained via the thermogravimetric analysis (TGA-DTA), which is one of the most commonly used techniques to study the primary reactions of thermal decomposition of solids.

2 EXPERIMENTAL

2.1 MATERIALS

The materials employed in this study were olive stones (OS), which are obtained from a Tunisian oleic manufacture. The precursor was naturally dried in the sun in order to reduce water content close to 10%. And then was grounded in order to have homogeneous products. After sieving, four sizes were selected for tests with particle diameter ranging from 0.63mm to 2.5mm ($0.63 < d < 1.25$ mm, $1.25 < d < 1.6$ mm, $1.6 < d < 2$ mm and $2 < d < 2.5$ mm). In the present study no physical or chemical treatment was undertaken.

Before thermogravimetric analysis, the samples were analyzed to determine the main properties that affect thermal conversion. Moisture content was determined gravimetrically by the oven drying method. Ultimate analysis was made in the institute for Agrobiotechnology Center for Analytical Chemistry (Austria). Proximate and chemical determinations were made according to standard analytical methods. The Higher Heat value (HHV) was determined using ultimate analysis [22]. The results are summarized in Table 1. They are in the same order of magnitude than results obtained in previous investigations ([5], [23]).

2.2 THERMOGRAVIMETRIC ANALYSIS (TGA)

Olive stones samples were subjected to thermogravimetric analysis using a SETARAM SETSYS EVOLUTION12 instrument controlled by a PC. Pyrolysis tests were performed in a Simultaneous differential thermogravimetric analyzer, TGA-DTA/DSC of Perkin Elmer under a Nitrogen atmosphere with a heat flow rate of 200 ml/min and an initial mass of sample around 25–30 mg. The sample weight loss and rate of weight loss as functions of time or temperature were recorded continuously under dynamic conditions. The reaction temperature range was 30-900 °C and the heating rate was controlled at 5, 10, 15 and 20 °C/min. The experiments were replicated three times to determine their reproducibility, and the average value was recorded. The experimental error of these measurements was calculated, obtaining an error for all studied samples of $\pm 0.5\%$ in weight loss measurement and ± 2 °C in temperature measurement.

2.3 KINETIC MODELING

Several approaches to kinetic analysis of thermogravimetric data have been used for the determination of the kinetic parameters for biomasses thermal degradation ([4], [8]).

In this paper, pyrolysis process was described by three different kinetic models, namely, the iso-conversional Kissinger–Akahira–Sunose (KAS) and Ozawa–Flynn–Wall (OFW) models ([19], [20], [21]), and Coats–Redfern model [8].

2.3.1 ISO-CONVERSIONAL MODELS

Iso-conversional methods are used for the determination of kinetic parameters without knowledge of reaction mechanism. These methods are model free and evaluate the activation energy at progressive values of conversion. These assumed that reaction kinetics does not relate with heating rate and the conversion of raw materials in a one-step process ([4], [25]).

The degree of conversion in pyrolysis reaction can be obtained by the following equation:

$$\alpha = \frac{w_0 - w}{w_0 - w_\infty} \quad (1)$$

Where w_0 , w and w_∞ refer to initial, instantaneous and final masses respectively.

The general non-isothermal decomposition reaction rate is expressed as:

$$\frac{d\alpha}{dt} = k(T)f(\alpha) \quad (2)$$

Where $f(\alpha)$ represents reaction model. $K(T)$ is the rate constant as expressed by Arrhenius equation as;

$$k(T) = A \exp\left(-\frac{E_a}{RT}\right) \quad (3)$$

Where A is the pre-exponential factor, E_a is the activation energy of the reaction, R is the universal gas constant, and T is the absolute temperature. By substituting Eq. (3) in Eq. (2) gives:

$$\frac{d\alpha}{dt} = A \exp\left(-\frac{E_a}{RT}\right) f(\alpha) \quad (4)$$

Taking into account that the temperature is a function of time and that it is increasing with a constant heating rate, β , the following expression is derived:

$$T = \beta t + T_0 \quad (5)$$

$$dT = \beta dt \quad (6)$$

Combining Eq. (4) and Eq. (6), and rearranging gives;

$$g(\alpha) = \int_0^\alpha \frac{d\alpha}{f(\alpha)} = \int_0^T \frac{A}{\beta} \exp\left(-\frac{E_a}{RT}\right) dT = \frac{AE_a}{\beta R} \int_x^\infty u^{-2} e^{-u} du = \frac{AE_a}{\beta R} P(x) \quad (7)$$

Where $x = E_a/RT$. The term $P(x)$ has no exact solution. Thus, Eq. (7) can be solved by numerical methods or approximations. The difference between the various iso-conversional methods is attributed to the type of approximation used.

2.3.1.1 THE KAS MODEL

The Kissinger–Akahira–Sunose (KAS) method introduces approximation [26] of:

$$P(x) = x^{-2} e^{-x} \quad (8)$$

into Eq. (7). After rearrangement, the expression becomes:

$$g(\alpha) = \frac{AE_a}{\beta R} x^{-2} e^{-x} \quad (9)$$

Expressing Eq. (9) in logarithmic form

$$\text{Ln}g(\alpha) = \text{Ln}\left(\frac{T^2}{\beta}\right) + \text{Ln}\left(\frac{AR}{E_a}\right) - \frac{E_a}{RT} \quad (10)$$

$$\text{Ln}\left(\frac{\beta}{T^2}\right) = \left[\ln\left(\frac{AE_a}{Rg(\alpha)}\right) \right] - \frac{E_a}{RT} \quad (11)$$

The slope of the curve $\text{Ln}\left(\frac{\beta}{T^2}\right)$ vs $1/T$, gives $-E_a/R$. By calculation in a conversion range from 0 to 1, activation energy for the progressing values of conversion can be calculated.

2.3.1.2 THE OFW MODEL

The Ozawa-Flynn-Wall method (OFW) method is based on Doyle's approximation ([4], [27]):

$$\log(P(x)) = -2.315 + 0.457x \quad (12)$$

By substituting Doyle's approximation into Eq. (7) and expressing in logarithm form:

$$\log(g(\alpha)) = \log\left(\frac{AE_a}{\beta R}\right) + \log(P(x)) \quad (13)$$

$$\log(\beta) = \log\left[\frac{AE_a}{Rg(\alpha)}\right] - 2.315 - 0.457 \frac{E_a}{RT} \quad (14)$$

The slope of the curve $\log(\beta)$ vs. $1/T$, gives $-E_a/R$. As mentioned before in KAS method, for range conversion from 0 to 1, activation energy for the progressing values of conversion can be calculated.

2.3.2 COATS REDFERN METHOD

Coats-Redfern method is a model free method that derived from Arrhenius equation [8]. Since the KAS and OFW methods are accurate enough for the calculation of the activation energy, the Coats-Redfern method will be used in order to calculate the pre-exponential factor, the apparent reaction order. The equations for the Coats-Redfern method are given by the following equation:

$$\frac{d\alpha}{dt} = k(T)(1-\alpha)^n \quad (15)$$

Rearranging and integrating Eq. (15), the following expression can be obtained:

$$\frac{1 - (1-\alpha)^{1-n}}{1-n} = \frac{A}{\beta} \int_0^T \exp\left(-\frac{E_a}{RT}\right) dT \quad (16)$$

$\int_0^T \exp\left(-\frac{E_a}{RT}\right) dT$ has no exact solution. $\exp(-E_a/RT)$ can be expressed as an asymptotic series and integrated, with ignoring the higher-order terms. Integration of this function gives,

$$\frac{1 - (1-\alpha)^{1-n}}{1-n} = \frac{ART^2}{\beta E_a} \left[1 - \frac{2RT}{E_a}\right] \exp\left(-\frac{E_a}{RT}\right) \quad (17)$$

Expressing Eq. (17) in logarithmic form gives:

$$\ln \left[\frac{1 - (1 - \alpha)^{1-n}}{T^2(1-n)} \right] = \ln \left[\frac{AR}{\beta E_a} \left(1 - \frac{2RT}{E_a} \right) \right] - \frac{E_a}{RT} \quad (\text{for } n \neq 1) \quad (18)$$

If assuming that $2RT/E_a \ll 1$ than Eq. (18) becomes

$$\ln \left[\frac{1 - (1 - \alpha)^{1-n}}{T^2(1-n)} \right] = \ln \left[\frac{AR}{\beta E_a} \right] - \frac{E_a}{RT} \quad (\text{for } n \neq 1) \quad (19)$$

If $n=1$, the following equation is to be used

$$\ln \left[\frac{\ln(1 - \alpha)}{T^2} \right] = \ln \left[\frac{AR}{\beta E_a} \left(1 - \frac{2RT}{E_a} \right) \right] - \frac{E_a}{RT} \quad (\text{for } n=1) \quad (20)$$

Thus a plot of

$$\ln \left[\frac{\ln(1 - \alpha)}{T^2} \right] \text{ versus } 1/T \quad \text{for } n \neq 1 \quad (21)$$

Or

$$\ln \left[\frac{1 - (1 - \alpha)^{1-n}}{T^2(1-n)} \right] \text{ versus } 1/T \quad \text{for } n=1 \quad (22)$$

Should result in a straight line of slope $-E_a/R$ the proper value of n . The values of α and T would be obtained from the TG analysis. The criterion used for acceptable values of E and A is that the final value of n should yield values of E whose linear correlation coefficients are the best.

3 RESULTS AND DISCUSSION

3.1 SAMPLES CHARACTERIZATION

The proximate and ultimate analyses of olive stones are shown in Table 1. A comparison of the obtained analysis results with common biomass is found. They are in the same order of magnitude than results obtained in previous investigations [5], [28], [29].

As seen in the basic analysis, the concentrations of C, H and O were similar to other common biomass that studied. Low nitrogen content is important because higher N percentages might be a problem for combustion processes, producing toxic NO_x emissions [4]. Nevertheless, S contents are null, implying fewer emissions or corrosion during utilization of these crops for power production.

Table 1 depicts also proximate analysis comparison of olive stones with other biomass. It can be seen that these materials have a high content of volatile matter and fixed carbon and low ash content, as well as other common biomass, which is interesting with respect to their applications in gasification and pyrolysis processes.

Table 1. Characteristics of olive stones (OS) and comparison with other biomass

Ultimate Analysis (wt %)	C	H	N	S	O*	References
OS	46.7	6.1	0.2	<0.2	47.0	This study
Orange Waste	47.00	6.90	01.3	0.09	44.71	[28]
Olive stone waste	57.62	8.08	01.34	0.17	27.73	[5]
Almond shell	50.50	6.60	0.20	0.01	42.69	[29]
Olive stone	44.80	6.00	0.10	0.01	49.09	[29]
Proximate Analysis (w%)	MC	VMC	FCC	AC	HHV(MJ/kg)	
OS	8.42	62.07	26.81	2.7	19.05	This study
Orange Waste	5.70	74.60	16.68	3.02	-	[28]
Almond shell	10.00	80.30	9.10	0.60	-	[29]
Olive stone	10.40	74.40	13.80	1.40	-	[29]
Olive stone waste	7.40	66.60	23.85	2.16	21.4	[5]

MC, moisture content; VMC, volatile matter content; AC, ash content; FCC, fixed carbon content;

* By difference

– Did not mention in the reference.

3.2 THERMOGRAVIMETRIC STUDY

The results of TGA analysis are shown in Fig. 1 which show the weight loss curves (TG) and derivative thermogravimetric (DTG) evolution profiles of olive stones, as a function of reaction temperature. According to this figure, thermograms of olive stones follow the usual shape for lignocellulosic materials [29]. Its thermal degradation can be divided into three stages; moisture drying, main degradation and continuous slight devolatilisation [4].

The first stage, namely the moisture drying region, is in temperature range from 300 to 480K as can be observed in Fig.1. In DTG profiles, it corresponds to the first significant peak. A mass loss of 9.6% is recorded and it is mainly attributed to release of weakly bonded water molecules [28].

The main degradation is located in the temperature range from 490 to 680K. This stage consist of a major loss of weight (52.33%) ascribed to hemicellulose and cellulose degradation.

On DTG curves, two distinct peaks are clearly observed, the first, occurring at lower temperatures, mainly corresponds to the hemicellulose decomposition. Because it's a mixture of various polymerized monosaccharides with lower degree of polymerization that the thermal stability was lower than cellulose ([13], [29]).

The main temperature degradation of hemicellulose was 523-595K associated with a weight loss of 24.52%.

The second peak (595-650K) was mainly attributed to the degradation of cellulose with a mass loss of 24%. It is mentioned that cellulose is a high-molecular compound with long linear chain composed of D-glucosyl group. And a part of cellulose has crystalline structure made of ordered microfibrils that resulted in thermal degradation more difficulty than hemicellulose ([13], [29]). The decomposition of these two polymers with the evolution of secondary gases remains a significant fraction of char [30].

However, it should be noted that although these two stages are mainly characterized by the decomposition of cellulose and hemicellulose, simultaneous degradation of lignin is also present at that temperature interval.

So, the third stage, with continuous slight devolatilisation at temperatures above 880K, corresponds to lignin decomposition. On DTG curves, a non-observable peak is indicated that it is known that lignin decompose slowly over a broader temperature. A prolonged and small mass loss was recorded (10.88%) and char was the main product from lignin degradation at the end of this stage.

Similar behavior was obtained for different biomasses ([7], [28], [29], [30]).

In summary, during the pyrolytic process of olive stones up to 900K, around 70% of the ligno-cellulosic biomass can be volatilized with a 30% of residual materials.

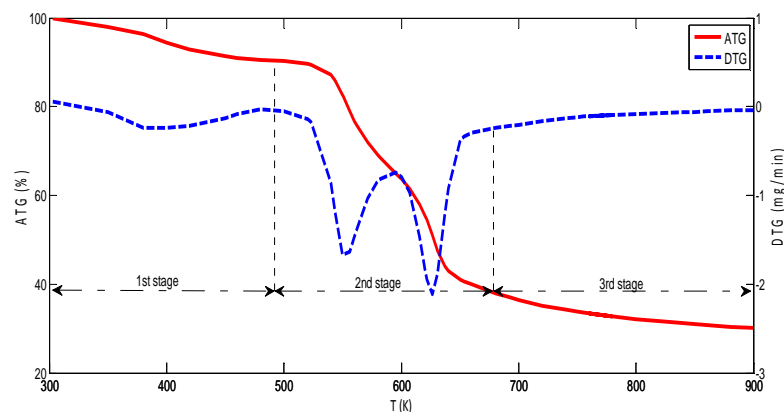


Fig. 1. TG and DTG curves of olive stones under inert atmosphere (10°C/min)

3.2.1 EFFECT OF HEATING RATES

Fig. 2 shows the DTG profiles of olive stones pyrolysis at different heating rates (5, 10, 15 and 20 °C/min).

Firstly, it can be seen that both points of maximum of mass loss rate in the DTG curves shifted toward higher temperatures. That's, increases in heating rate tended to delay the thermal degradation processes towards higher temperatures. This behavior could be attributed to heat transfer limitations with increasing heating rates ([30], [31]). At lower heating rates, heating of biomass particles occurs more gradually and leads a better heat transfer to the interior of biomass [32].

Secondly, it can be seen that the maximum mass loss rate increases with respect to the heating rates. This behavior is most probably due to a higher amount of thermal energy which promoted the heat transfer between the surrounding and interior the biomass samples [33]. However, the amount of formed char was not affected noticeably with heating rates between 5°C/min and 20°C/min. This behavior has been previously described by other researches ([32], [33]).

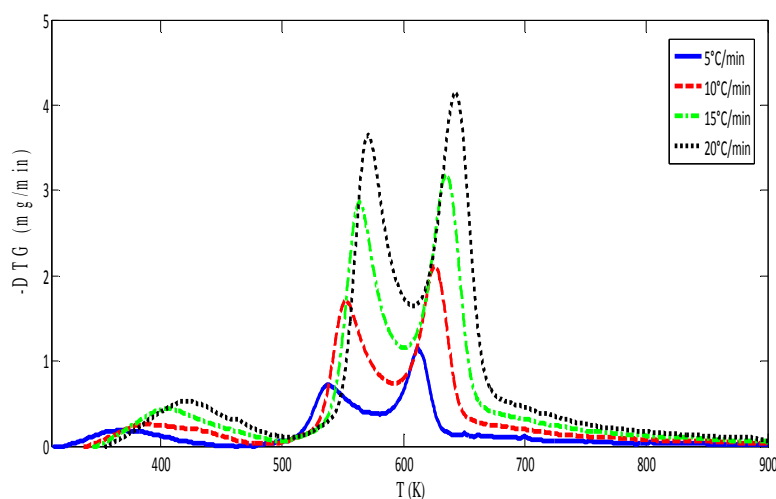


Fig. 2. Effect of heating rate on olive stone pyrolysis profiles (N_2)

3.2.2 EFFECT OF PARTICLE SIZE

The influence of the particle size was also studied for three different particle sizes of OS ($d < 0.5\text{mm}$; $1 < d < 1.5\text{mm}$; $2 < d < 2.8\text{mm}$) under inert atmosphere. The TG curves reported in Fig. 3 shows that particles diameter have no effect on obtained experiments data. It could be due to the size of particle that's small enough to not cause effects of heat and mass transfer resistance inside the particle. These results were obtained by several researches [34]. Guo and Lua [8] reported that pyrolysis is controlled by pure reaction kinetics for the samples size smaller than 2 mm.

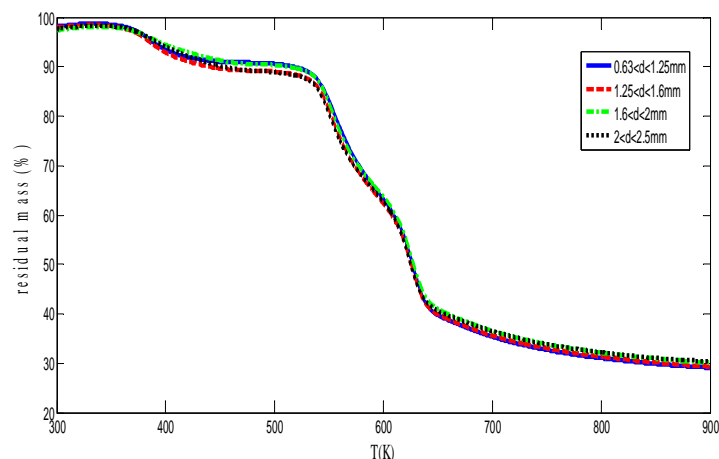


Fig. 3. Effect of particle size on olive stone TG pyrolysis profiles (10°C/min; N₂)

3.3 KINETIC ANALYSIS

3.3.1 EVALUATION OF ACTIVATION ENERGY USING ISO-CONVERSIONAL MODELS

The kinetic parameters of olive stones pyrolysis were calculated by iso-conversional KAS and OFW models. Activation energy can be calculated from the slope of the Arrhenius plot.

According to KAS model, based on Eq. (8), activation energy, can be determined from the relationship between $\ln(\beta/T^2)$ and $1/T$ (Eq. (8)). Fig. 4a shows linear plot of $\ln(\beta/T^2)$ versus $1/T$ at various conversions from 10% to 90%, resulting in a family of parallel straight lines with a slope of $-E/R$. Using OFW method, activation energy has been obtained from the slope of linear plot of $\ln \beta$ versus the inverse temperature at different rates conversion (Fig.4b).

The obtained activation energies (E) using KAS and OFW methods, as well as the respective correlation factors (R^2) are listed in Table 2. It can be seen that the determination coefficients are close to unit for all cases, indicating good fitting results. The values of E_a calculated by the two iso-conversional methods presented a great accordance with a deviation below 10% for rate conversion above 0.2. However, this is not the case with the activation energies at small conversion values.

The small differences among the activation energy values are due to the difference in approximations used to calculate the temperature integral in these methods. This agreement validates the reliability of calculations and confirmed the predictive power of KAS and OFW methods [28].

As seen from Table 2, the activation energy values increased with conversion. The difference between the lowest and highest activation energy value from two models close to 50-60 kJ/mol for conversion values ranging from 0.2 to 0.8 (depending on conversion). These means that OS pyrolysis is a complex process progresses through multi-step kinetics with various apparent activation energies [4]. The variation in reaction mechanism causes changes in E values with progressing conversion.

For more precision, the variation of activation energies as a function of conversion degrees is shown in Fig. 5 for two models. We take the values of the KAS model as an example. It's clear that above 10%, activation energy presented low value. up to the conversion of 20%, the activation energy increased from 20 kJ/mol to 80 kJ/mol. Then, it increased slowly from 85 to 139 kJ/mol with increasing the conversion from 20% to 50%. In the conversion ranges 50%-70%, apparent energy maintained the similar values (about 138 kJ/mol). Above 80%, the activation energy increased sharply.

As shown in the TG and DTG curves (Fig.1), the moisture on the surfaces OS sample vaporized below 440 K. It was assumed that the activation energy of 20 kJ/mol at 10% conversion corresponded to the vaporization of moisture.

Fisher et al. [35] studied the pyrolysis of cellulose using TGA at different heating rates. They reported that DTG curves occurred between 573 K and 673 K. As seen in Fig.1, main peaks in DTG curves were below 670 K, which could be corresponding to cellulose and hemicellulose. Then, cellulose and hemicellulose decomposed up to the conversion of 70%.

In the other hand, Vamvuka et al. [30] reported that the activation energies for cellulose, hemicelluloses and lignin are in the range of 145–285 kJ/mol, 90–125 kJ/mol and 30–39 kJ/mol, respectively. It was also reported that activation energy of

hemicellulose pyrolysis is lower than the activation energy of cellulose pyrolysis ([11], [36]). The values at lower conversions can be attributed to hemicellulose. Then, it was assumed that the activation energy ranged from 85 to 125 kJ/mol, for conversion between 20 and 40 % corresponded to the hemicellulose decomposition. And the activation energy of the value around 140kJ/mol for conversion range 50-70% corresponded to cellulose decomposition.

The increase of activation energy at higher conversion was explicated differently in literature. Park et al. [11] attributed this phenomenon to further devolatilization reaction of char after the main reaction. Liang et al. [37] reported that it could be caused by the influence of heat transfer at high temperatures. Otherwise, Lopez-Velazquez et al. [28] shows that this interval was attributed to the last stage degradation of lignin.

Most of cellulose and hemicelluloses were decomposed at the pyrolytic conversion from 20% to 70% with the average activation energy of 121.2 kJ/mol.

Vamvuka et al. [30] reported that the activation energies for cellulose and hemicelluloses are in the range of 145–285 kJ/mol, 90–125 kJ/ mol, respectively. Lopez-Velazquez et al. [28] studied the pyrolysis of orange waste and show that observed activation energy values are in the range 120–250 kJ/mol for conversion interval 20-80%. The average apparent energy for the Pinyon pine was 108 kJ/mol for conversion between 10% and 80 % [33].

On the other hand, Park et al. [11] studied the pyrolysis kinetics of oak trees. They said that the average activation energy, having a value of 236 kJ/mol, showing higher values compared to the literature.

In general, we can deduce that the variation in apparent activation energy for OS pyrolysis showed similar trend as the reported data.

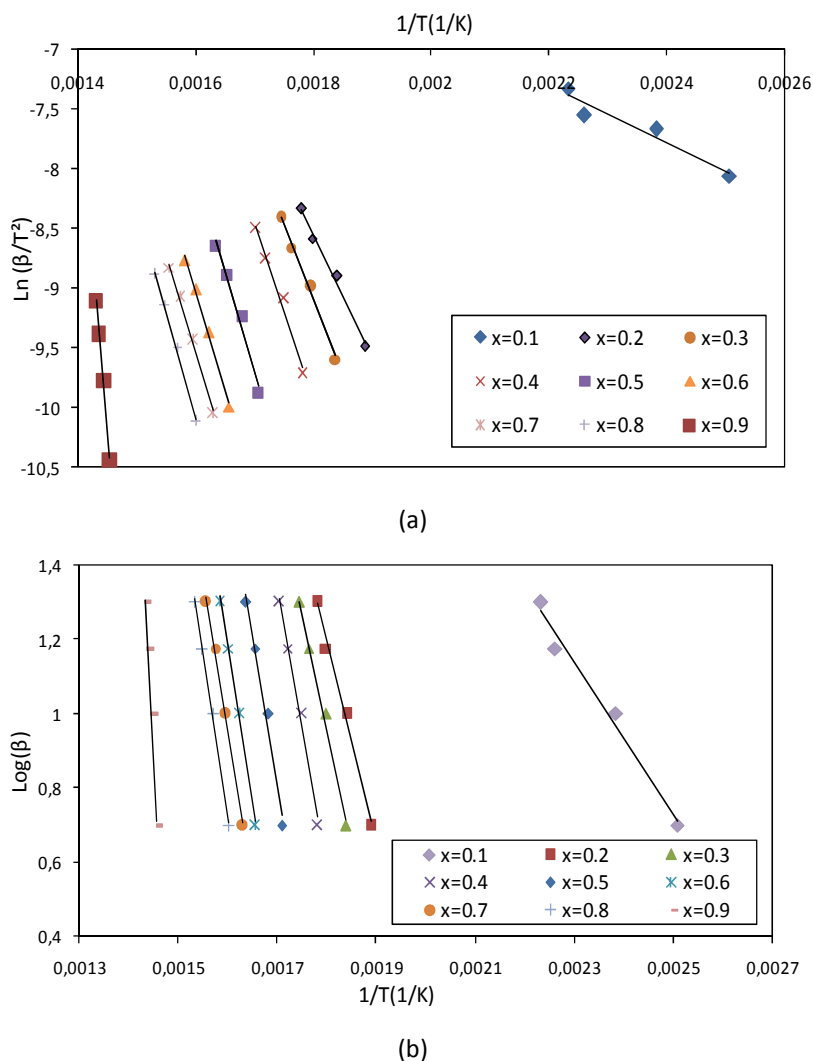


Fig. 4. Estimation of activation energy using the KAS (a) and OFW (b) methods for olive stones pyrolysis.

Table 2. TGA pyrolysis of OS activation energies (E_a) and correlation factors (R^2) for different conversion values using KAS and OSW models

Conversion(x)	E_a ; KAS model ; kJ/mol	R^2	E_a ; OFW model ; kJ/mol	R^2	%difference
0.1	19.496	0.932	37.854	0.982	48.49
0.2	85.351	0.989	98.367	0.993	3.23
0.3	102.337	0.99	114.503	0.993	10.62
0.4	125.059	0.982	136.134	0.986	8.13
0.5	139.159	0.979	149.633	0.983	7
0.6	138.486	0.993	149.088	0.995	7.11
0.7	137.222	0.996	147.941	0.997	7.24
0.8	146.052	0.998	156.419	0.998	6.62
0.9	471.736	0.994	466.366	0.995	-1.15

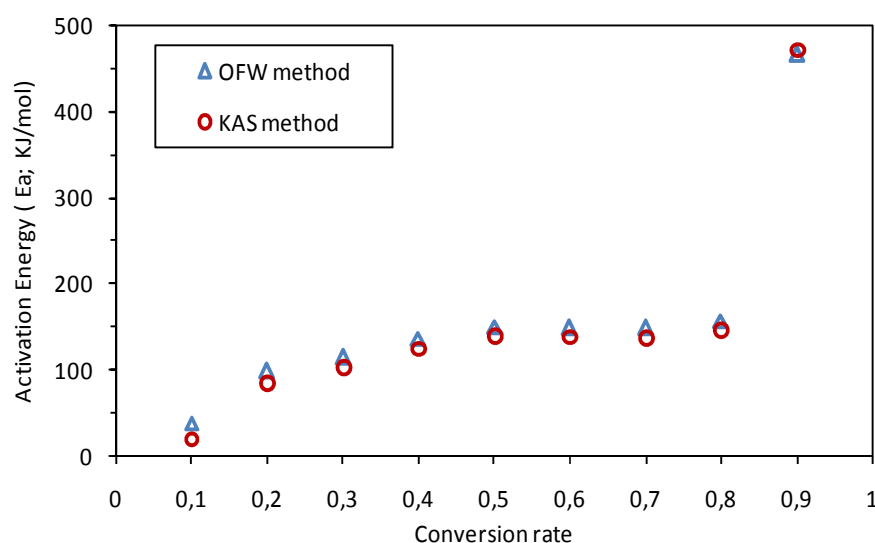


Fig. 5. Activation energy distribution at different conversion rates determined from KAS and OFW methods.

3.3.2 KINETIC MODELLING USING ISO-CONVENTIONAL MODELS

In order to evaluate the pyrolysis of olive stones, the pre-exponential factor (A) had to be determined. For this, the Coats-Redfern method has been used, as described elsewhere in this work and two cases were examined: the case where the whole phenomenon can be simulated as a single pseudo-reaction of varying pseudo-order and the case where pyrolysis is considered as a single first order reaction. The mean activation energies calculated by KAS and OFW methods will be used for the determination of the pre-exponential factors for every case. The mean activation energy used is the average of rate conversion interval 0.2-0.8. Conversion degrees below 0.2 and above 0.8 does not included because of the stability of activation energy values and to reduce the effect of moisture and ash on activation energy ([4], [37]).

Fig. 6 shows a simulation of the pyrolysis of olive stones by solving Eq. (4) for heating rate 5°C/min, using the obtained values from the KAS method coupled with the Coats-Redfern model.

These values of obtained parameters are listed in Table 3 along with the average activation energy, obtained from two methods.

For different heating rates, the variable order method ($n \neq 1$) shows an overall better accordance with the values obtained from TGA.

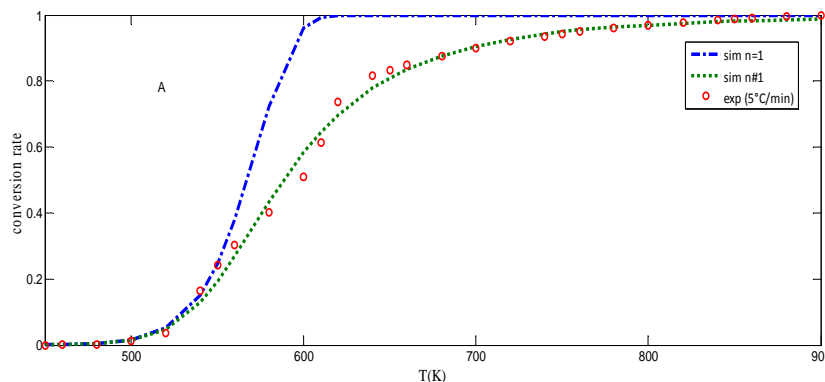


Fig. 6. Simulation of OS pyrolysis using the kinetic data calculated from the KAS method (5°C/min).

Table 3. Calculated activation energies (E) and pre-exponential factors (A) for Olive stones using the KAS and OFW iso-conversional methods

	KAS				OFW			
$E(\text{KJ/mol})$	124.81				136,01			
$\beta(^{\circ}\text{C/min})$	5	10	15	20	5	10	15	20
$A(\text{min}^{-1})$	5.10^{10}	$4.11.10^{10}$	5.10^{10}	$4.02.10^{10}$	1.12^{10}	$4.11.10^{10}$	$3.5.10^{11}$	$5.0.10^{11}$
n	3.53	3.024	3.06	2.80	4.28	3.10	2.83	3.17

4 CONCLUSION

In this study the thermal degradation of olive stones has been investigated via thermogravimetric analysis.

The thermal behavior was divided into three stages; moisture drying, main degradation and continuous slight devolatilisation

The DTG plot show that olive stones degradation occurred in the temperature range of 480-680 K and exhibits two major peaks. The first peak could be generated by the decomposition of hemicellulose. The second peak should correspond to the decomposition of cellulose. As heating rate is increased from 5 to 20 °C/min, the decomposition process is shifted to higher temperature zone. While, different particles sizes (<2.5mm) don't have any effect on the pyrolysis of olive stones.

The activation energy distribution was obtained. At low conversions (below 0.15), E was below 30 kJ/ mol. In the conversion of 0.20–0.80, E was between 85 and 140 kJ/mol above rate conversion 0.8, E increased rapidly and reach above 400 kJ/mol.

Three kinetic models, the iso-conversional Kissinger-Akahira-Sunose (KAS), Ozawa-Flynn-Wall (OFW) models and Coats Redfern method were used to calculate the kinetic parameters. All models are in good agreement with the experimental data. However, the dependence of the apparent activation energy on the conversion degree reveals that pyrolysis progress rather through multi-steps kinetics.

REFERENCES

- [1] K.R Duarte, C. Justino, T. Panteleitchouk, A. Zrineh, A.C. Freitas, A.C. Duarte, "Removal of phenolic compound in olivemill wastewater by silica–alginate–fungi biocomposites", J. Environ. Sci. Technol, 2013.
- [2] I. Karaouzas, E. Cotou, T. Albanis, A. Kamarianos, N. Skoulikidis, U. Giannakou, "Bioassays and biochemical biomarkers for assessing olive mill and citrus processing, wastewater toxicity", Environ. Toxic, vol. pp. 26, 669–76, 2011.
- [3] R. Lahyani, L.C. Coelho, M. Khemakhem, G. Laporte, F. Semet, "Applications A multi-compartment vehicle routing problem arising in the collection of olive oil inTunisia", Omega, vol. 51, pp. 1-10, 2015.
- [4] Th. Damartzis, D. Vamvuka, S. Sfakiotakis, A. Zabaniotou, "Thermal degradation studies and kinetic modeling of cardoon (*Cynara cardunculus*) pyrolysis using thermogravimetric analysis (TGA)", Bioresour. Technol, vol. 102, pp. 6230-6238, 2011.

- [5] A. Chouchène, M. Jeguirim, B. Khiari, F. Zagrouba, G. Trouvé, "Thermal degradation of olive solid waste: Influence of particle size and oxygen concentration", *Resour. Conserv. Recy*, vol. 54, pp. 271–27, 2010.
- [6] G. Várhegyi, J.A. Michael, E. Jakab, P. Szabó, "Kinetic modeling of biomass pyrolysis", *J. Anal. Appl. Pyrol*, vol. 42, pp. 73–87, 1997.
- [7] A. Agrawal, S. Chakraborty, "A kinetic study of pyrolysis and combustion of microalgae *Chlorella vulgaris* using thermogravimetric analysis", *Bioresour. Technol.*, vol. 128, pp. 72–80, 2013.
- [8] J. Guo, A.C. Lua, "Kinetic study on pyrolytic process of oil palm solid waste using two step consecutive reaction model", *Biomass Bioenergy*, vol. 20, pp. 223–233, 2001.
- [9] O.A. Akinwale, F.G. Johann, M. Carrier, L.M. Edson, J.H. Knoetze, "Thermogravimetric study of the pyrolysis characteristics and kinetics of coal blends with corn and sugarcane residues", *Fuel Process. Technol*, vol. 106, pp. 310–320, 2013.
- [10] A. Ounas, A.Aboulkas, K. El harfi, A. Bacaoui, A. Yaacoubi, "Pyrolysis of olive residue and sugar cane bagasse: Non-isothermal thermogravimetric kinetic analysis", *Bioresour. Technol*, vol. 102, pp. 11234–11238, 2011.
- [11] Y-H. Park, J. Kim, S-S. Kim, Y-K. Park, "Pyrolysis characteristics and kinetics of oak trees using thermogravimetric analyzer and micro-tubing reactor", *Bioresour. Technol*, vol.100, pp. 400-405, 2009.
- [12] C. David, S. Salvador, J.L. Dirion, M. Quintard, "Determination of a reaction scheme for cardboard thermal degradation using thermal gravimetric analysis", *J. Anal. Appl. Pyrol*, vol. 67, pp. 307-323, 2003.
- [13] Z. Ma, D. Chen, J. Gu, B. Bao, Q. Zhang, "Determination of pyrolysis characteristics and kinetics of palm kernel shell using TGA–FTIR and model-free integral methods", *Energy Convers. Manage*, vol. 89, pp. 251-259, 2015.
- [14] S. Ceylan, Y. Topcu, Z. Ceylan, "Thermal behaviour and kinetics of alga *Polysiphonia elongata* biomass during pyrolysis", *Bioresour. Technol*, vol. 171, pp. 193-198, 2014.
- [15] S-S. Kim, H.V. Ly, J. Kim, J.H. Choi, H.C. Woo, "Thermogravimetric characteristics and pyrolysis kinetics of *Alga Sagarssum* sp", *Biomass. Bioresour Technol*, vol. 139, pp. 242- 248, 2013.
- [16] M. Lajili, L. Limousy, M. Jeguirim, "Physico-chemical properties and thermal degradation characteristics of agropellets from olive mill by-products/sawdust blends", *Fuel Process. Technol*, vol. 126, pp. 215–221, 2014.
- [17] A. Zabaniotou, Th. Damartzis, "Modelling the intra-particle transport phenomena and chemical reactions of olive kernel fast pyrolysis", *J. Anal. Appl. Pyrol*, vol. 80, pp. 187–194, 2007.
- [18] J.A. Caballero, J.A. Conesa, R. Font, A. Marcilla, "Pyrolysis kinetics of almond shells and olive stones considering their organic fractions", *J. Anal. Appl. Pyrol*, vol. 42, pp. 159-175, 1997.
- [19] J.H. Flynn, A.L. Wall, "A quick direct method for determination of activation energy from thermogravimetric data", *J. Polym. Sci., Part B: Polym. Phys.*, vol. 323, pp. 8, 1966.
- [20] T. Ozawa, "A new method of analyzing thermogravimetric data", *Bull Chem Soc Jpn*, vol. 38, pp. 1881-6, 1965.
- [21] H.E. Kissinger, "Reaction kinetics in differential thermal analysis", *Anal. Chem.*, vol. 29, pp. 1702–6, 1957.
- [22] C. Sheng, J.L.T. Azevedo, "Estimating the higher heating value of biomass fuels from basic analysis data", *Biomass Bioenergy*, vol. 28, pp. 499-507, 2005.
- [23] O. Senneca, "Kinetics of pyrolysis, combustion and gasification of three biomass fuels", *Fuel Process. Technol*, vol. 88, pp. 87-97, 2007.
- [24] J.H. Flynn, "The isoconversional method for determination of energy of activation at constant heating rates: Corrections of the Doyle Approximation", *J. Therm. Anal. Calorim*, vol. 27, pp. 95-102, 1983.
- [25] S.S. Idris, N. Abd Rahman, K. Ismail, "Combustion characteristics of Malaysian oil palm biomass, sub-bituminous coal and their respective blends via thermogravimetric analysis (TGA)", *Bioresour. Technol*, vol. 123, pp. 581-591, 2012.
- [26] N. Sbirrazzuoli, L. Vincent, J. Bouillard, L. Elegant, "Isothermal and non isothermal kinetics when mechanistic information available", *J. Therm. Anal*, vol. 56, pp. 783-792, 1999.
- [27] C.D. Doyle, "Series approximations to the equations of thermogravimetric data *Nature*", vol. 207, pp. 290-291, 1965.
- [28] M.A. Lopez-Velazquez, V. Santes, J. Balmaseda, E. Torres-Garcia, "Pyrolysis of orange waste: A thermo-kinetic study", *J. Anal. Appl. Pyrol*, vol. 99, pp. 170-177, 2013.
- [29] J.F. Gonzalez, S. Roman, J.M. Encinar, G. Martinez, "Pyrolysis of various biomass residues and char utilization for the production of activated carbons". *J. Anal. Appl. Pyrol*, vol. 58, pp. 134-141, 2009.
- [30] D. Vamvuka, E. Kakaras, E. Kastanaki, P. Grammelis, "Pyrolysis characteristics and kinetics of biomass residuals mixtures with lignite". *Fuel*, vol. 82, pp. 1949–1960, 2003.
- [31] S.S. Idris, N. Abd Rahman, K. Ismail, A.B. Alias, Z. Abd Rashid, M.J. Aris, "Investigation on thermochemical behaviour of low rank Malaysian coal, oil palm biomass and their blends during pyrolysis via thermogravimetric analysis (TGA)", *Bioresour. Technol*, vol. 101, pp. 4584-4592, 2010.
- [32] S. Ceylan, Y. Topcu, "Pyrolysis kinetics of hazelnut husk using thermogravimetric analysis", *Bioresour. Technol*, vol. 156, pp. 182-188, 2014.

- [33] S-S. Kim, A. Shenoy, F.A. Agblevor, "Thermogravimetric and kinetic study of Pinyon pine in the various gases", *Bioresour Technol*, vol. 156, pp. 297–302, 2014.
- [34] P. Weerachanchai, C. Tangsathitkulchai, M. Tangsathitkulchai, "Comparison of pyrolysis kinetics models for thermogravimetric analysis of biomass". *J. Sci. Technol*, vol. 17, pp. 378-400, 2010.
- [35] T. Fisher, M. Hajaligol, B. Waymack, D. Kellogg, "Pyrolysis behavior and kinetics of biomass derived materials", *J. Anal. Appl. Pyrol*, vol. 62, pp. 331-349, 2002.
- [36] A. Anca-Couce, A. Berger, N. Zobel, "How to determine consistent biomass pyrolysis kinetics in a parallel reaction scheme", *Fuel*, vol.123, pp. 230–240, 2014.
- [37] Y. Liang, B. Cheng, Y. Si, D. Cao, H. Jiang, G. Han, X. Liu, "Thermal decomposition kinetics and characteristics of *Spartina alterniflora* via thermogravimetric analysis", *Renew. Energy*, vol. 68, pp. 111-117, 2014.